

## Experimental Full Network Nonlocality with Independent Sources and Strict Locality Constraints

Xue-Mei Gu<sup>1,2,3</sup>, Liang Huang<sup>1,2,3</sup>, Alejandro Pozas-Kerstjens<sup>4,5</sup>, Yang-Fan Jiang<sup>6</sup>, Dian Wu<sup>1,2,3</sup>,  
Bing Bai<sup>1,2,3</sup>, Qi-Chao Sun<sup>1,2,3</sup>, Ming-Cheng Chen<sup>1,2,3</sup>, Jun Zhang<sup>1,2,3</sup>, Sixia Yu<sup>1</sup>, Qiang Zhang<sup>1,2,3</sup>,  
Chao-Yang Lu<sup>1,2,3</sup> and Jian-Wei Pan<sup>1,2,3</sup>

<sup>1</sup>Hefei National Research Center for Physical Sciences at the Microscale and School of Physical Sciences, University of Science and Technology of China, Hefei 230026, China

<sup>2</sup>Shanghai Research Center for Quantum Science and CAS Center for Excellence in Quantum Information and Quantum Physics, University of Science and Technology of China, Shanghai 201315, China

<sup>3</sup>Hefei National Laboratory, University of Science and Technology of China, Hefei 230088, China

<sup>4</sup>Instituto de Ciencias Matemáticas (CSIC-UAM-UC3M-UCM), 28049 Madrid, Spain

<sup>5</sup>Departamento de Análisis Matemático, Universidad Complutense de Madrid, 28040 Madrid, Spain

<sup>6</sup>Jinan Institute of Quantum Technology, Jinan 250101, China



(Received 29 June 2022; revised 5 February 2023; accepted 31 March 2023; published 11 May 2023)

Nonlocality arising in networks composed of several independent sources gives rise to phenomena radically different from that in standard Bell scenarios. Over the years, the phenomenon of network nonlocality in the entanglement-swapping scenario has been well investigated and demonstrated. However, it is known that violations of the so-called *bilocal inequality* used in previous experimental demonstrations cannot be used to certify the nonclassicality of their sources. This has put forward a stronger concept for nonlocality in networks, called full network nonlocality. Here, we experimentally observe full network nonlocal correlations in a network where the source-independence, locality, and measurement-independence loopholes are closed. This is ensured by employing two independent sources, rapid setting generation, and spacelike separations of relevant events. Our experiment violates known inequalities characterizing nonfull network nonlocal correlations by over 5 standard deviations, certifying the absence of classical sources in the realization.

DOI: [10.1103/PhysRevLett.130.190201](https://doi.org/10.1103/PhysRevLett.130.190201)

Bell's theorem [1], stating that quantum predictions are incompatible with local realism, has deeply influenced our understanding of physics. Specifically, the correlations obtained by local measurements on a remotely shared quantum system cannot be explained by a local hidden variable (LHV) model. This is generally known as Bell nonlocality [2], which has been confirmed in numerous Bell experiments [3–7] via violations of Bell inequalities [1,8]. Apart from its fundamental interest, Bell nonlocality has also found numerous applications as an indispensable resource in device-independent quantum information tasks [9–11].

In the standard Bell tests for LHV models, local influences are mediated by a single, common LHV that is shared among all the parties. Recently, growing interest has been devoted to the exploration of Bell nonlocality in networks (see Ref. [12] for a recent review). The simplest example is the entanglement-swapping scenario [13], where two independent parties that are not causally connected can become entangled. While correlations generated in networks can be contrasted against standard LHV models, it is more natural and physically motivated to consider models with independent hidden variables that

reproduce the network structure. In the entanglement-swapping network, this gives rise to the study of bilocal hidden variable (BLHV) models and the associated phenomenon of (non)-bilocality [14,15]. Importantly, recent experiments [16–20] show that there are correlations that admit a standard LHV model but nonetheless are incompatible with a BLHV model [depicted in Fig. 1(a)].

It was recently argued that the violation of the inequalities characterizing correlations with BLHV models did not capture all the intricacies of nonlocality in the entanglement-swapping network [21]. Concretely, the bilocal inequality in [15] can be violated when just one of the sources is entangled [17]. More importantly, all its quantum violations can be simulated with a strategy of the form depicted in Fig. 1(b), that is, keeping one classical source if the other one is allowed to distribute systems only limited by the no-signaling principle (e.g., a Popescu-Rohrlich box [22] that allows stronger-than-quantum correlations) [21]. These systems are currently a hypothetical construct, but it is useful to consider them in order to be able to make statements independent of the theory describing the physical systems involved [23,24].

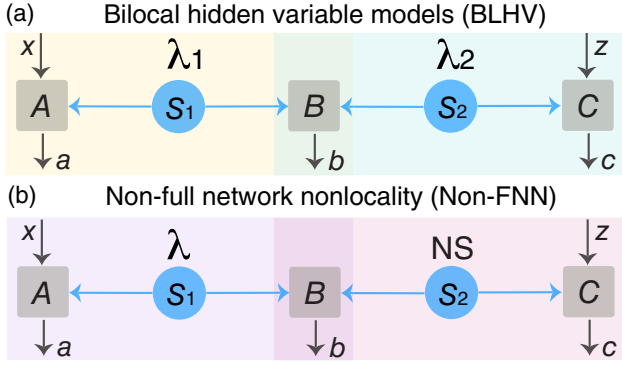


FIG. 1. A network with sources (blue circles) distributing physical systems (blue arrows) to three nodes Alice, Bob, and Charlie, represented as  $A$ ,  $B$ , and  $C$  (gray squares).  $(x, a)$  and  $(z, c)$  are Alice's and Charlie's inputs and outputs. Bob performs a joint measurement on his systems yielding outcomes  $b$ . (a) BLHV model, where each source distributes a different LHV ( $\lambda_1$  and  $\lambda_2$ ). (b) Test for FNN, where the model to be discarded consists of one LHV  $\lambda$  and a general nonlocal source (NS).

In other words, a violation of the bilocality inequality only guarantees that at least one of the sources in the network is nonclassical. In order to have a device-independent certification that both sources are nonclassical, one must (i) insert the additional hypothesis that quantum mechanics describes nature at its fundamental level and (ii) achieve a violation of the bilocality inequality beyond the value described in [17]. But if the additional assumption (i) is removed, no value of the inequality guarantees the absence of classical sources in the network.

This put forward a stronger, arguably more genuine, definition of network nonlocality, where distributions regarded as interesting are those that cannot be explained by having at least one classical source, regardless of the rest. This is known as full network nonlocality (FNN) [21], and its observation implies that all the sources used in the network must necessarily uphold some degree of nonclassicality. FNN has been since then observed in experimental realizations of the entanglement-swapping scenario featuring three- [25] and four-outcome [26] measurements in the central party, and in the three-branch star network [27]. Importantly, the independence of the sources in these experiments is assumed rather than enforced. This opens the possibility of the existence of an LHV simulation of the correlations observed [28], known as the *source independence loophole*. Similarly, the independence of the measurement choices and the isolation of the parties are also assumed, leading to the *freedom of choice* and the *locality* loopholes, respectively.

Here, we report the first experimental demonstration of the existence of FNN in quantum theory in a realization where the network structure is strictly guaranteed. This is, we show that there exist probability distributions generated in quantum networks that cannot be simulated if one of the sources distributes classical systems, even if the rest are

allowed to distribute (so far, hypothetical) stronger-than-quantum systems. We do so by violating the FNN witnesses of [21] in an optical network that distributes quantum systems generated from independent sources under strict locality conditions, i.e., in which all the parties involved are spacelike separated.

*FNN in the entanglement-swapping network.*—FNN correlations are defined, analogously to standard nonlocal ones, as not admitting a specific model. In the entanglement-swapping scenario, this model is captured in Fig. 1(b). The correlations generated when the source  $S_1$  is classical (i.e., an LHV) are described by  $p(a, b, c|x, z) = \int d\lambda \rho(\lambda) p(a|x, \lambda) p(b, c|\lambda, z)$ , where  $\rho(\lambda)$  is the probability distribution characterizing the LHV  $\lambda$  between Alice and Bob,  $p(a|x, \lambda)$  is Alice's response function, and  $p(b, c|\lambda, z)$  is a joint response function for Bob and Charlie, which in general is only constrained by no signaling [i.e., by  $\sum_c p(b, c|\lambda, z) = p(b|\lambda)$  and  $\sum_b p(b, c|\lambda, z) = p(c|z)$ ]. To establish FNN, one needs to consider also the case with interchanged sources. Reference [21] showed that, in the entanglement-swapping scenario when  $a, c, z, x \in \{0, 1\}$  and  $b \in \{0, 1, 2\}$ , the simultaneous violation of both the following inequalities certifies FNN:

$$\mathcal{R}_{C-NS} := 2\langle A_0 B_1 (C_0 - C_1) \rangle + \langle A_1 B_0 (2C_0 + C_1) \rangle - \langle B_0 \rangle + (\langle A_1 B_0 \rangle + \langle B_0 C_0 \rangle - \langle C_0 \rangle) \langle C_1 \rangle \leq 3, \quad (1)$$

and

$$\mathcal{R}_{NS-C} := 2\langle A_0 B_1 (C_0 - C_1) \rangle + \langle A_1 B_0 (C_0 + 2C_1) \rangle - \langle B_0 \rangle + \langle A_1 \rangle (\langle A_1 B_0 \rangle + \langle B_0 C_1 \rangle + \langle C_0 - C_1 - A_1 \rangle) \leq 3, \quad (2)$$

where expectation values are computed following [15], namely,  $\langle A_x B_0 C_z \rangle = \sum_{a,b,c} (-1)^{a+c+|b|} p(a, b, c|x, z)$  and  $\langle A_x B_1 C_z \rangle = \sum_{a,b \in \{0,1\}, c} (-1)^{a+b+c} p(a, b, c|x, z)$ , the function  $[p]$  evaluating to 0 if  $p$  is true and to 1 otherwise (see Ref. [29] for further details).

Importantly, these inequalities can be violated simultaneously in quantum networks [ [21], App. F]. Take both sources to emit a Bell state  $|\Phi^+\rangle$ , Alice and Charlie to perform measurements  $A_x \in \{X, Z\}$  and  $C_z \in \{[(Z+X)/\sqrt{2}], [(Z-X)/\sqrt{2}]\}$ , where  $X$  and  $Z$  are the Pauli operators, and Bob to perform a partial Bell state measurement (BSM) with three outputs  $\{\Phi^+, \Phi^-, \mathbb{1} - \Phi^+ - \Phi^-\}$  that are correspondingly associated to the outcomes  $b \in \{0, 1, 2\}$ , where  $\Phi^\pm = |\Phi^\pm\rangle\langle\Phi^\pm|$ . The resulting distribution  $p(a, b, c|x, z)$  leads to the violations  $\mathcal{R}_{C-NS} = \mathcal{R}_{NS-C} = 5/\sqrt{2} \approx 3.5355$ .

*Experimental realization.*—We implement this in a photonic network, illustrated in Fig. 2(a). Two independent sources  $S_1$  and  $S_2$  distribute entangled photons to three separate

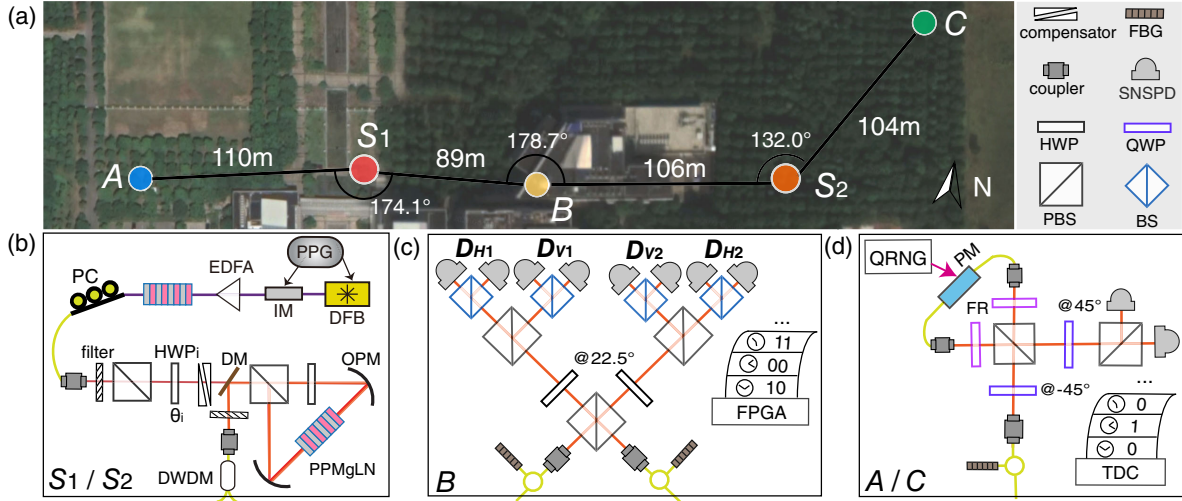


FIG. 2. Experimental realization. (a) Overview of our quantum network with two independent sources ( $S_1$  and  $S_2$ ) and three nodes (Alice, Bob, and Charlie, represented as  $A$ ,  $B$ , and  $C$ ). Geographic picture is taken from Google Maps, ©2022 Google [35]. (b) By pumping a periodically poled MgO doped lithium niobate (PPMgLN) crystal in a Sagnac loop, photon pairs in the state  $|\varphi\rangle_i = \cos 2\theta_i|HH\rangle + \sin 2\theta_i|VV\rangle$  are created via SPDC in each source, where  $\theta_i$  is the angle of the HWP $_i$  mounted on a motorized rotator. The pulse pattern generator (PPG) in  $S_1$  acts as a master clock for synchronizing all devices (see Refs. [19,34] for details). (c) Bob performs a partial Bell state measurement [36] and his photon detection events are real-time analyzed and recorded by a field-programmable gate array (FPGA). (d) Alice and Charlie measure their photons according to the inputs from their private quantum random number generators (QRNGs). Their detection events and setting choices are recorded by a time-to-digital converter (TDC). See Ref. [29] for more details. IM, intensity modulator; EDFA, erbium-doped fiber amplifier; PC, polarization controller; DM, dichroic mirror; OPM, off-axis parabolic mirror; DWDM, dense wavelength-division multiplexer; FBG, fiber Bragg grating; PBS, polarizing beam splitter; HWP, half-wave plate; QWP, quarter-wave plate; BS, beam splitter; SNSPD, superconducting nanowire single photon detector; FR, Faraday rotator; PM, electro-optic phase modulator.

observers Alice, Bob, and Charlie. Each source generates a polarization-entangled state  $|\varphi\rangle_i = \cos 2\theta_i|HH\rangle + \sin 2\theta_i|VV\rangle$  via type-0 spontaneous parametric down-conversion (SPDC), as shown in Fig. 2(b). In each source, a pulse pattern generator (PPG) sends 250 MHz trigger signals to drive a distributed feedback (DFB) laser such that its electric current switches from much below to well above the lasing threshold, indicating that the phase of each generated pump pulse is randomized [33]. In this way, we erase any quantum coherence between the pump pulses and disconnect the two SPDC processes on each experimental trial, thus closing the source-independence loophole under the reasonable assumption that hidden variables are created together with state emission (further details see Refs. [19,34]).

At the central node, Bob sandwiches polarization beam splitters (PBSs) between two half-wave plates (HWP at  $22.5^\circ$ ) to realize a partial BSM [36] that distinguishes Bell states  $|\Phi^+\rangle$ ,  $|\Phi^-\rangle$ , and a remaining group of Bell states  $\{|\Psi^+\rangle, |\Psi^-\rangle\}$  (which is  $1 - \Phi^+ - \Phi^-$ ) by the coincidence detection among the pseudo-number-resolving detectors depicted as  $D_{H1}$ ,  $D_{V1}$ ,  $D_{H2}$ , and  $D_{V2}$  in Fig. 2(c). Bob's photon detections are analyzed in real time and recorded by a field-programmable gate array. Once Bob obtains a BSM output, he sends the corresponding timestamp information to Alice and Charlie. We implement a high-speed, high-fidelity, single-photon polarization analyzer at a rate of

250 MHz at Alice's and Charlie's location [Fig. 2(d)], where the measurement choice depends on random bits produced from private fast quantum random number generators (QRNGs) [29]. All random bits from the QRNGs pass the NIST randomness tests [37] (for more details, see Refs. [19,34,38]). All setting results and detections are locally recorded by their time-to-digital converters that are fed with Bob's timestamps information. All locally stored data are collected by a separate computer, in which we postselect the four-photon coincidences "by aligning all of them to Bob's BSM timestamps and use the four-photon coincidences for  $\mathcal{R}_{C-NS}$  and  $\mathcal{R}_{NS-C}$ ."

We confirm the space-time configuration and characterize the delays of all relevant events, namely, (1) emission ( $S_1$  and  $S_2$ ), i.e., the photon creation events in the sources; (2) the choice of measurement setting (QRNG $_A$  and QRNG $_C$ ), i.e., completing the quantum random number generation at Alice's and Charlie's nodes for choosing their measurements; and (3) the measurement ( $M_A$ ,  $M_B$ , and  $M_C$ ), i.e., finishing the single photon detection by Alice, Bob, and Charlie. In the experiment, the time reference to synchronize all events is set to the 12.5 GHz internal microwave clock of the PPG in source  $S_1$  [34]. By employing QRNG and spacelike separating setting choice and measurement on one side from the measurement on other sides, we close the locality loophole. By spacelike

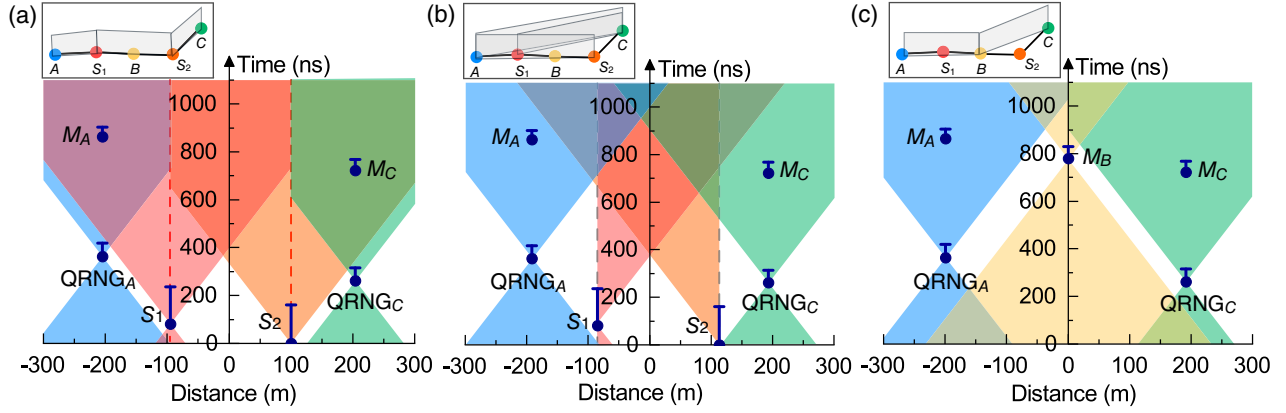


FIG. 3. Space-time configuration in each experimental trial. (a)–(c) Space-time diagrams of the relationship between important events in the nodes, as displayed in the boxes. Blue vertical bars in each space-time diagram denote the time elapsing for the relevant events, with start and end marked by circles and horizontal lines, respectively. (a) Left, middle, and right panels split by red dashed lines: space-time analysis between  $QRNG_A$  and  $S_1$ , space-time analysis between  $S_1$  and  $S_2$ , and space-time analysis between  $S_2$  and  $QRNG_C$ . (b) Space-time analysis between  $QRNG_A$  and  $QRNG_C$ , and spacelike separations between  $QRNG_A$  ( $QRNG_C$ ) and  $M_C$  ( $M_A$ ), and between  $S_1$  ( $S_2$ ) and  $M_C$  ( $M_A$ ). (c) Space-time analysis between  $M_B$  and  $QRNG_A$  ( $QRNG_C$ ). All the space-time relations are drawn to scale. For more details see Ref. [29].

separating setting choice events from state creation events (which is also the origin of a hidden variable), we also close the measurement-independence loophole. Finally, the emission at  $S_1$  is spacelike separated from Charlie’s

measurement, and analogously for Alice’s measurement and the emission at  $S_2$ . The details about the spacelike separation of all relevant events are shown in Fig. 3 and [29].

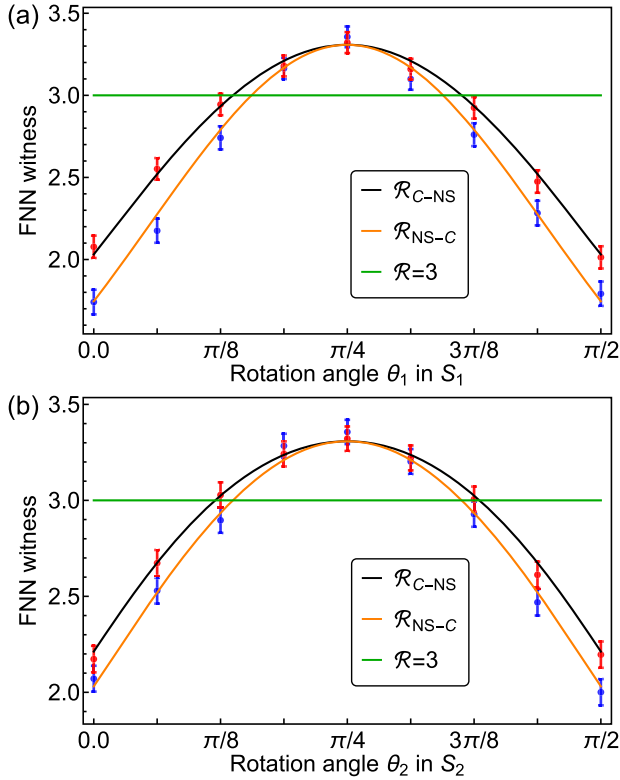


FIG. 4. Experimental results of the FNN witness as functions of the rotation angle  $\theta_i$  in  $S_i$ . (a) FNN witness as a function of the angle  $\theta_1$  when  $|\varphi\rangle_2 = |\Phi^+\rangle$ . (b) FNN witness as a function of the angle  $\theta_2$  when  $|\varphi\rangle_1 = |\Phi^+\rangle$ . Error bars indicate one standard deviation.

*Results.*—We obtain visibilities of  $(97.10 \pm 0.35)\%$  and  $(98.60 \pm 0.07)\%$  for states  $|\Phi^+\rangle$  generated in the diagonal polarization basis for sources  $S_1$  and  $S_2$ , respectively, at an average photon pair number per pulse of  $\sim 0.007$ . The Hong-Ou-Mandel measurement by Bob yields a fitted visibility of  $(94.3 \pm 2.7)\%$ . We then study the distributions  $p(a, b, c|x, z)$  generated in our network with different states computing their corresponding values of  $\mathcal{R}_{C-NS}$  and  $\mathcal{R}_{NS-C}$  [29]. For simplicity, we fix one source creating  $|\Phi^+\rangle$  and then automatically rotate the phase  $\theta_i$  in the other source with a motorized rotator at a phase interval of  $\pi/16$ , having a total of nine steps within the range  $[0, \pi/2]$ . For each step, we collect  $\sim 4700$  four-photon coincidence detection events in  $\sim 10\,000$  seconds, and compute with them the results shown in Fig. 4. Our observation of  $\mathcal{R}_{C-NS} > 3$  in Fig. 4(a) certifies that  $S_1$  distributes an entangled quantum system to Alice and Bob. An analogous argument applies for  $S_2$  and Eq. (2) in Fig. 4(b). But more importantly, the fact that in Fig. 4(a) we observe a simultaneous violation of both inequalities for the points  $\theta_1 = 3\pi/16, \pi/4$  and  $5\pi/16$  is, at least in those cases, a guarantee that both sources in the network are nonclassical. The same conclusions can be obtained when changing the state in  $S_2$  as we show in Fig. 4(b). Notably, in the particular case of  $|\varphi\rangle_1 = |\varphi\rangle_2 = |\Phi^+\rangle$ , our results yield  $\mathcal{R}_{C-NS} = 3.3212 \pm 0.0638$  and  $\mathcal{R}_{NS-C} = 3.3563 \pm 0.0632$  both in Figs. 4(a) and 4(b), surpassing the non-FNN’s bound by more than 5 standard deviations.

*Discussion.*—We have experimentally demonstrated the existence of FNN in a photonic quantum network built upon sharing independent sources under strict locality

constraints. FNN is witnessed by the simultaneous violation of Eqs. (1) and (2). Each violation certifies, in a device-independent manner, that one of the sources in the network is not classical. Thus, our experiment constitutes a certification of the nonclassicality of all the sources in the entanglement-swapping scenario. Importantly, the fact that non-FNN models consider general no-signaling systems implies that, even in the hypothetical case that new physical systems were discovered that allowed for stronger-than-quantum correlations, it would remain impossible to reproduce the results of our experiments by using these systems in one source and classical systems in the other. This is a very important feature for quantum communication networks. In contrast with pioneering work [28] which requires all the sources to distribute stronger-than-quantum systems in order to limit the information accessible by an eavesdropper, FNN could provide a strong, yet achievable in quantum theory, way of guaranteeing security of network-based quantum cryptographic protocols.

Our experiment addresses the source-independence, locality, and measurement-independence loopholes, thus providing a strong certification of FNN. However, it remains subject to the detection loophole, namely, that a local model could be given if taking into account non-detection events [39], and the memory loophole, by which the results in a given experimental round may depend on the previous ones [40,41]. These loopholes need to be closed in order for the certification to be considered device independent [5]. The former could be addressed in the future by using high-efficiency photon sources [42] and detectors, while closing the latter requires suitable hypothesis testing [41,43] and sufficiently many experimental rounds, thus benefiting from higher-frequency hardware. Beyond the bilocal scenarios, an important direction is to explore FNN in more complex networks such as star scenarios [44–46] where several independent branch parties are connected to a central one, and line scenarios that underlie long-distance quantum communication networks.

We thank Chang Liu and Quantum Ctek for providing the components used in the quantum random number generators. This work was supported by the National Key Research and Development Program of China (2020YFA0309704), Shandong Provincial Natural Science Foundation (ZR2021LLZ005), the National Natural Science Foundation of China (12004138), the Chinese Academy of Sciences, the National Fundamental Research Program, the Anhui Initiative in Quantum Information Technologies, the Spanish Ministry of Science and Innovation MCIN/AEI/10.13039/501100011033 and the European Union NextGenerationEU/PRTR (CEX2019-000904-S and PID2020-113523GB-I00), the Spanish Ministry of Economic Affairs and Digital Transformation (project QUANTUM ENIA), Comunidad de Madrid (QUITEMAD-CM P2018/TCS-4342), Universidad

Complutense de Madrid (FEI-EU-22-06), and the CSIC Quantum Technologies Platform PTI-001.

X.-M. G., L. H., and A. P. K. contributed equally to this work.

- 
- [1] J. S. Bell, *Phys. Phys. Fiz.* **1**, 195 (1964).
  - [2] N. Brunner, D. Cavalcanti, S. Pironio, V. Scarani, and S. Wehner, *Rev. Mod. Phys.* **86**, 419 (2014).
  - [3] L. K. Shalm, E. Meyer-Scott, B. G. Christensen, P. Bierhorst, M. A. Wayne, M. J. Stevens, T. Gerrits, S. Glancy, D. R. Hamel, M. S. Allman *et al.*, *Phys. Rev. Lett.* **115**, 250402 (2015).
  - [4] M. Giustina, M. A. N. Versteegh, S. Wengerowsky, J. Handsteiner, A. Hochrainer, K. Phelan, F. Steinlechner, J. Kofler, J.-Å. Larsson, C. Abellán *et al.*, *Phys. Rev. Lett.* **115**, 250401 (2015).
  - [5] B. Hensen, H. Bernien, A. E. Dréau, A. Reiserer, N. Kalb, M. S. Blok, J. Ruitenberg, R. F. Vermeulen, R. N. Schouten, C. Abellán *et al.*, *Nature (London)* **526**, 682 (2015).
  - [6] W. Rosenfeld, D. Burchardt, R. Garthoff, K. Redeker, N. Ortegel, M. Rau, and H. Weinfurter, *Phys. Rev. Lett.* **119**, 010402 (2017).
  - [7] M.-H. Li, C. Wu, Y. Zhang, W.-Z. Liu, B. Bai, Y. Liu, W. Zhang, Q. Zhao, H. Li, Z. Wang *et al.*, *Phys. Rev. Lett.* **121**, 080404 (2018).
  - [8] J. F. Clauser, M. A. Horne, A. Shimony, and R. A. Holt, *Phys. Rev. Lett.* **23**, 880 (1969).
  - [9] A. Acín, N. Brunner, N. Gisin, S. Massar, S. Pironio, and V. Scarani, *Phys. Rev. Lett.* **98**, 230501 (2007).
  - [10] A. Acín and L. Masanes, *Nature (London)* **540**, 213 (2016).
  - [11] S. Pironio, A. Acín, S. Massar, A. Boyer de La Giroday, D. N. Matsukevich, P. Maunz, S. Olmschenk, D. Hayes, L. Luo, T. A. Manning *et al.*, *Nature (London)* **464**, 1021 (2010).
  - [12] A. Tavakoli, A. Pozas-Kerstjens, M.-X. Luo, and M.-O. Renou, *Rep. Prog. Phys.* **85**, 056001 (2022).
  - [13] J.-W. Pan, D. Bouwmeester, H. Weinfurter, and A. Zeilinger, *Phys. Rev. Lett.* **80**, 3891 (1998).
  - [14] C. Branciard, N. Gisin, and S. Pironio, *Phys. Rev. Lett.* **104**, 170401 (2010).
  - [15] C. Branciard, D. Rosset, N. Gisin, and S. Pironio, *Phys. Rev. A* **85**, 032119 (2012).
  - [16] G. Carvacho, F. Andreoli, L. Santodonato, M. Bentivegna, R. Chaves, and F. Sciarrino, *Nat. Commun.* **8**, 14775 (2017).
  - [17] D. J. Saunders, A. J. Bennet, C. Branciard, and G. J. Pryde, *Sci. Adv.* **3**, e1602743 (2017).
  - [18] F. Andreoli, G. Carvacho, L. Santodonato, M. Bentivegna, R. Chaves, and F. Sciarrino, *Phys. Rev. A* **95**, 062315 (2017).
  - [19] Q.-C. Sun, Y.-F. Jiang, B. Bai, W. Zhang, H. Li, X. Jiang, J. Zhang, L. You, X. Chen, Z. Wang *et al.*, *Nat. Photonics* **13**, 687 (2019).
  - [20] D. Poderini, I. Agresti, G. Marchese, E. Polino, T. Giordani, A. Suprano, M. Valeri, G. Milani, N. Spagnolo, G. Carvacho *et al.*, *Nat. Commun.* **11**, 2467 (2020).
  - [21] A. Pozas-Kerstjens, N. Gisin, and A. Tavakoli, *Phys. Rev. Lett.* **128**, 010403 (2022).
  - [22] S. Popescu and D. Rohrlich, *Found. Phys.* **24**, 379 (1994).

- [23] N. Gisin, J.-D. Bancal, Y. Cai, P. Remy, A. Tavakoli, E. Zambrini Cruzeiro, S. Popescu, and N. Brunner, *Nat. Commun.* **11**, 2378 (2020).
- [24] X. Coiteux-Roy, E. Wolfe, and M.-O. Renou, *Phys. Rev. Lett.* **127**, 200401 (2021).
- [25] E. Håkansson, A. Piveteau, S. Muhammad, and M. Bourennane, [arXiv:2201.06361](https://arxiv.org/abs/2201.06361).
- [26] C.-X. Huang, X.-M. Hu, Y. Guo, C. Zhang, B.-H. Liu, Y.-F. Huang, C.-F. Li, G.-C. Guo, N. Gisin, C. Branciard, and A. Tavakoli, *Phys. Rev. Lett.* **129**, 030502 (2022).
- [27] N.-N. Wang, A. Pozas-Kerstjens, C. Zhang, B.-H. Liu, Y.-F. Huang, C.-F. Li, G.-C. Guo, N. Gisin, and A. Tavakoli, *Nat. Commun.* **14**, 2153 (2023).
- [28] C. M. Lee and M. J. Hoban, *Phys. Rev. Lett.* **120**, 020504 (2018).
- [29] See Supplemental Material at <http://link.aps.org/supplemental/10.1103/PhysRevLett.130.190201> for analytical calculations on the bounds of Eqs. (1) and (2) and further experimental details. It includes Refs. [15,21,23,30–32].
- [30] E. Wolfe, R. W. Spekkens, and T. Fritz, *J. Causal Infer.* **7** (2019).
- [31] E. Wolfe, A. Pozas-Kerstjens, M. Grinberg, D. Rosset, A. Acín, and M. Navascués, *Phys. Rev. X* **11**, 021043 (2021).
- [32] J. D. Jackson, *Classical Electrodynamics* (Wiley, New York, 1999), pp. 527–529.
- [33] C. Abellán, W. Amaya, D. Mitrani, V. Pruneri, and M. W. Mitchell, *Phys. Rev. Lett.* **115**, 250403 (2015).
- [34] D. Wu, Y.-F. Jiang, X.-M. Gu, L. Huang, B. Bai, Q.-C. Sun, X. Zhang, S.-Q. Gong, Y. Mao, H.-S. Zhong, M.-C. Chen, J. Zhang, Q. Zhang, C.-Y. Lu, and J.-W. Pan, *Phys. Rev. Lett.* **129**, 140401 (2022).
- [35] <https://www.google.com/maps/@31.1269385,121.5420419,644a,35y,350.24h/data=!3m1!1e3>.
- [36] J.-W. Pan and A. Zeilinger, *Phys. Rev. A* **57**, 2208 (1998).
- [37] L. E. Bassham, A. Rukhin, J. Soto, J. Nechvatal, M. Smid, E. Barker, S. Leigh, M. Levenson, M. Vangel, D. Banks, A. Heckert, J. Dray, and S. Vo, A statistical test suite for random and pseudorandom number generators for cryptographic applications (2010), NIST Special Publication 800-22 rev. 1a, <https://www.nist.gov/publications/statistical-test-suite-random-and-pseudorandom-number-generators-cryptographic>.
- [38] Y. Liu, Q. Zhao, M.-H. Li, J.-Y. Guan, Y. Zhang, B. Bai, W. Zhang, W.-Z. Liu, C. Wu, X. Yuan *et al.*, *Nature (London)* **562**, 548 (2018).
- [39] P. M. Pearle, *Phys. Rev. D* **2**, 1418 (1970).
- [40] L. Accardi and M. Regoli, Locality and Bell’s inequality, in *Foundations of Probability and Physics* (World Scientific, Singapore, 2001), pp. 1–28, [10.1142/9789812810809\\_0001](https://doi.org/10.1142/9789812810809_0001).
- [41] J. Barrett, D. Collins, L. Hardy, A. Kent, and S. Popescu, *Phys. Rev. A* **66**, 042111 (2002).
- [42] H. Wang, Y.-M. He, T.-H. Chung, H. Hu, Y. Yu, S. Chen, X. Ding, M.-C. Chen, J. Qin, X. Yang *et al.*, *Nat. Photonics* **13**, 770 (2019).
- [43] R. D. Gill, Accardi contra Bell (cum mundi): The Impossible Coupling, [arXiv:quant-ph/0110137](https://arxiv.org/abs/quant-ph/0110137).
- [44] A. Tavakoli, P. Skrzypczyk, D. Cavalcanti, and A. Acín, *Phys. Rev. A* **90**, 062109 (2014).
- [45] F. Andreoli, G. Carvacho, L. Santodonato, R. Chaves, and F. Sciarrino, *New J. Phys.* **19**, 113020 (2017).
- [46] A. Tavakoli, M.-O. Renou, N. Gisin, and N. Brunner, *New J. Phys.* **19**, 073003 (2017).